

Myosin VI targeting to clathrin-coated structures and dimerization is mediated by binding to Disabled-2 and PtdIns(4,5)P₂

Giulietta Spudich¹, Margarita V. Chibalina², Josephine Sui-Yan Au¹, Susan D. Arden², Folma Buss² and John Kendrick-Jones^{1,3}

Vesicle transport is essential for the movement of proteins, lipids and other molecules between membrane compartments within the cell. The role of the class VI myosins in vesicular transport is particularly intriguing because they are the only class that has been shown to move ‘backwards’ towards the minus end of actin filaments¹. Myosin VI is found in distinct intracellular locations and implicated in processes such as endocytosis^{2,3}, exocytosis, maintenance of Golgi morphology^{4,5} and cell movement⁶. We have shown that the carboxy-terminal tail is the key targeting region and have identified three binding sites: a WWY motif for Disabled-2 (Dab2) binding, a RRL motif for glucose-transporter binding protein (GIPC) and optineurin binding and a site that binds specifically and with high affinity ($K_d = 0.3 \mu\text{M}$) to PtdIns(4,5)P₂-containing liposomes. This is the first demonstration that myosin VI binds lipid membranes. Lipid binding induces a large structural change in the myosin VI tail (31% increase in helicity) and when associated with lipid vesicles, it can dimerize. *In vivo* targeting and recruitment of myosin VI to clathrin-coated structures (CCSs) at the plasma membrane is mediated by Dab2 and PtdIns(4,5)P₂ binding.

Dab2 is a myosin VI-binding partner present on endocytic CCSs at the plasma membrane^{7,8}. To establish whether binding to Dab2 is involved in targeting myosin VI to CCSs an extensive series of myosin VI tail-deletion fragments and point mutants were examined using the mammalian two-hybrid assay⁷. A relatively conservative single-amino-acid change from tryptophan to leucine (W1184L, WWY→WLY) was found to abolish myosin VI binding to Dab2 (Fig. 1a). Pull-down experiments using GST-tagged wild-type myosin VI tail or tail containing the WWY→WLY mutation, together with *in vitro* translated Dab2, confirmed the identity of the Dab2 binding site (Fig. 1c). To determine whether the Dab2 binding site was essential for targeting myosin VI to CCSs *in vivo*, GFP-tagged mutant tail constructs were overexpressed in HeLa cells.

Myosin VI containing a mutated Dab2-binding site (WWY→WLY) was not targeted to CCSs (Fig. 1d, e). It was previously shown^{2,8} that the presence of a large insert just before the globular carboxy-terminal domain (see Supplementary Information, Fig. S1), in conjunction with Dab2 binding, was also required for targeting myosin VI to CCSs at the plasma membrane.

GIPC is another myosin VI binding partner⁹ that is found in both clathrin-coated¹⁰ and uncoated endocytic vesicles³. To examine the involvement of GIPC in targeting myosin VI to CCSs, the GIPC binding site on the myosin VI tail was mapped by deletion and alanine-scanning mutagenesis. Mutation of RRL to AAA in the C-terminal tail domain (amino acids 1107–1109; Fig. 1b) abolished GIPC binding, but had no effect on Dab2 binding (Fig. 1a, b). Optineurin, a myosin VI binding protein associated with the Golgi complex and secretion, also specifically binds to the RRL binding site in the myosin VI tail⁴. Although phosphorylation of the threonines in the TINT sequence 15 residues upstream of RRL (see Supplementary Information, Fig. S1b) regulated optineurin binding to the RRL site⁴, TINT phosphorylation had no effect on GIPC binding to this site (data not shown).

As a number of endocytic and actin cytoskeleton proteins (such as AP-2, Dab2, gelsolin and cofilin) bind to phospholipids, we examined whether the myosin VI tail would bind lipids. ‘Mixed-brain’ liposomes were incubated with full-length myosin VI tail, C-terminal globular tail fragment, and full-length myosin VI (with Ca²⁺) and these proteins were present in the lipid pellet fraction after centrifugation, indicating strong lipid binding (Fig. 2a, b). Without liposomes, all the myosin VI constructs remained in the supernatant after centrifugation. To map the lipid-binding region, myosin VI-tail constructs were tested for liposome binding using the sedimentation assay (Fig. 2c). Although amino-terminal helical-tail fragments with and without the large insert (NT + LI, NT) scored a low but significant level of homology with the lipid binding Bin–amphiphysin–Rvs (BAR) domain of D-amphiphysin (Peter, B. & McMahon, H., unpublished observations), they did not

¹MRC Laboratory of Molecular Biology, Hills Road, Cambridge CB2 2QH, UK. ²Cambridge Institute for Medical Research, University of Cambridge, Wellcome/MRC Building, Hills Road, Cambridge CB2 2XY, UK.

³Correspondence should be addressed to J.K.-J. (e-mail: jkj@mrc-lmb.cam.ac.uk)

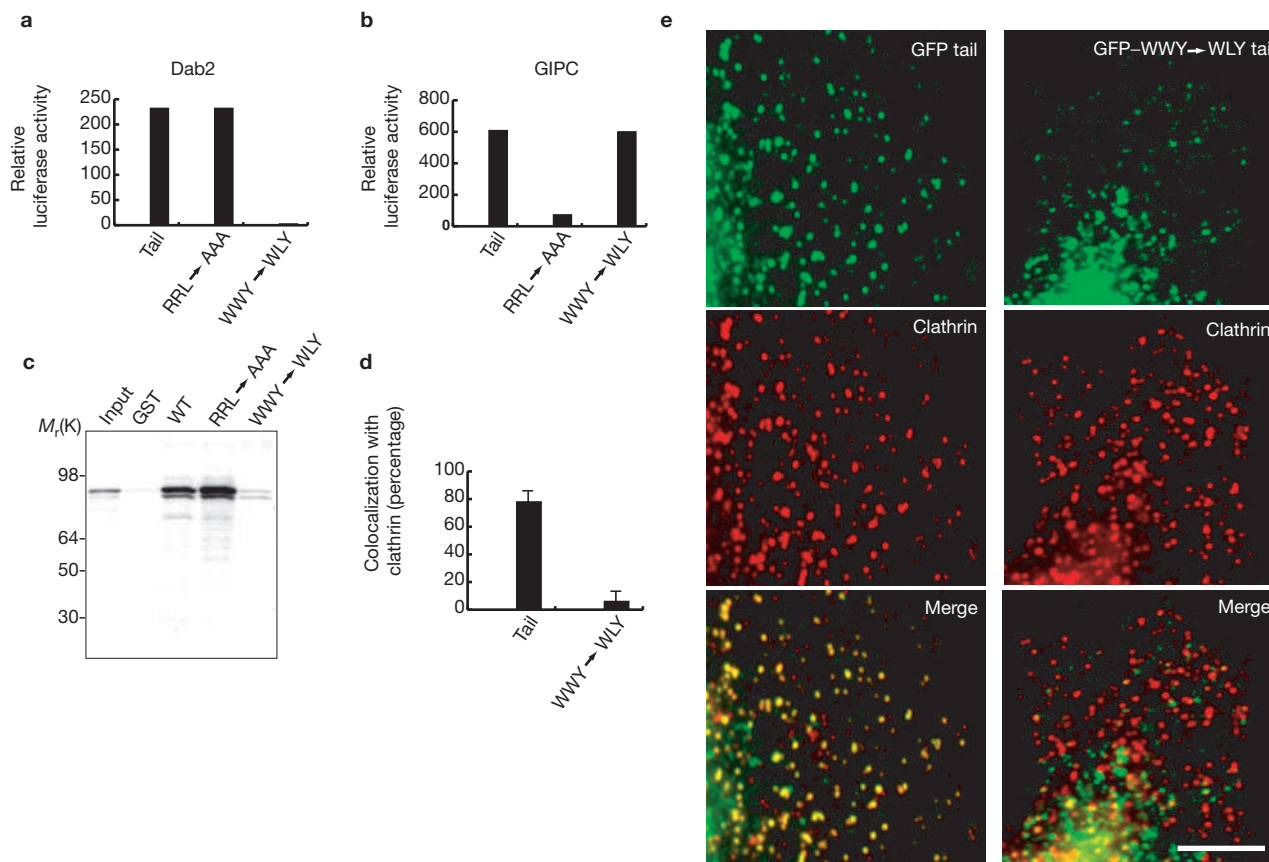


Figure 1 Two distinct 'hot spots' for binding Dab2 and GIPC were identified on the myosin VI tail. **(a, b)** Deletion and mutated constructs of the chicken myosin VI tail were screened for binding to Dab2 and GIPC using the mammalian two-hybrid system. The mutation W1184L (WWY→WLY) in the tail abolishes binding to Dab2, while preserving binding to GIPC. Mutation of the GIPC binding site (amino acids 1107–1109, RRL→AAA) abolishes GIPC binding in addition to optineurin binding but has no effect on Dab2 binding. These results indicate that there are two distinct sites for binding partners on the myosin VI tail. **(c)** Autoradiograph of ^{35}S -labelled Dab2 pull-down fractions. Recombinant, purified GST-tagged myosin VI tail containing the WWY→WLY mutation does not bind ^{35}S -labelled Dab2, whereas GST-tagged myosin VI tail (both wild-type and containing the mutations for GIPC

and/or optineurin binding; RRL→AAA) bound to ^{35}S -labelled Dab2. GST alone was included as a control. **(d)** Quantification of the colocalization of endogenous clathrin with GFP-tagged myosin VI tail (+LI; both wild-type and Dab2-binding mutant) by measuring the immunofluorescence staining shown in **e**. Myosin VI containing the mutated Dab2 binding site (WWY→WLY) does not colocalize with clathrin. **(e)** Immunofluorescence microscopy of overexpressed GFP-labelled myosin VI whole tail (+LI) constructs and endogenous clathrin in HeLa cells. Dab2 binding is required for targeting the myosin VI isoform with the large insert (+LI) to clathrin-coated pits and vesicles. Note the tail with the WWY→WLY mutation localizes to punctate structures, but as they are not clathrin-coated vesicles they are probably secretory or uncoated vesicles. The scale bar represents 5 μm .

bind to liposomes. Similarly, a construct comprising the last 142 amino acids of the C-terminal tail (amino acids 1134–1276; see Supplementary Information, Fig. S1) did not bind liposomes (Fig. 2c). Therefore, we searched for potential liposome-binding sequences between amino acids 1059 and 1134 in the myosin VI C-terminal tail. Deletion of this 75 amino acid region ($\Delta\text{PtdIns}(4,5)\text{P}_2$ tail) resulted in a 70% reduction in lipid binding. Within this region there is a stretch of basic and/or hydrophobic residues (RRLKVYHAWKSKNKKR, amino acids 1107–1122), but a series of single point mutations made in the basic residues had no effect on liposome binding, nor did double mutations in this region (data not shown). However, both myosin VI C-terminal tail and whole-tail constructs containing four point mutations in this region (WKSKNKKR→WASANNR, amino acids 1115–1122) had severely reduced liposome binding (by at least 70%; Fig. 2c).

We examined the structural organization of the C-terminal cargo-binding domain of myosin VI using limited proteolysis. Similarly to the myosin V C-terminal tail¹⁶, the myosin VI C-terminal domain is

extremely susceptible to tryptic digestion, rapidly yielding two fragments (bands 1 and 2 in Fig. 2d). Sequence analysis revealed that cleavage occurred at R1122 (see Supplementary Information, Fig. S1b, site 1), producing fragments with relative molecular masses of 18,000 and 11,000 (M_r 18K and 11K, respectively; bands 1 and 2 in Fig. 2d) that can be separated under non-dissociating conditions (see Methods). In the presence of liposomes, the tryptic cleavage pattern is different; cleavage does not occur at R1122, but at K1132 (band 3 in Fig. 2d and Supplementary Information, Fig. S1b, site 2) presumably because lipid binding to the potential binding site (KSKNKKR) protects site 1 from tryptic cleavage. In the lipid binding assay, the 11K fragment (domain 2) binds to liposomes, whereas the 18K fragment (domain 1) does not (Fig. 2e), confirming the identity of the lipid-binding region previously established in the mutational analysis (Fig. 2c).

When lipid binding to full-length myosin VI was tested, myosin VI only bound to liposomes in the presence of calcium (Fig. 2b). As calcium does not seem to affect lipid binding to the myosin VI tail or tail fragments,

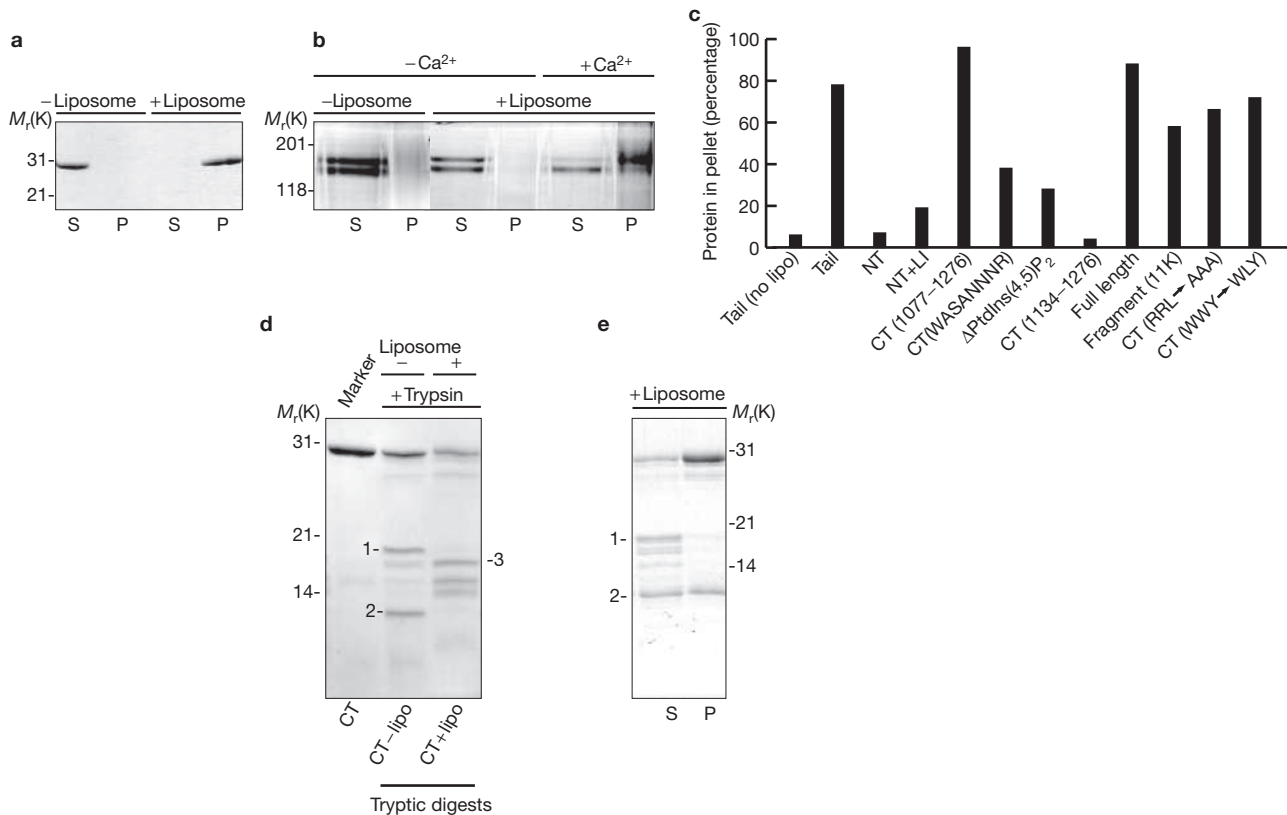


Figure 2 The C-terminal half of the myosin VI tail binds to liposomes and is composed of two independent domains. **(a)** The C-terminal half of the tail without the large insert (CT) binds liposomes. The CT tail (amino acids 1077–1276) is in the pellet (P) plus liposomes, and in the supernatant (S) without liposomes. **(b)** Full-length myosin VI binds to liposomes only in the presence of calcium (0.3 mM free Ca²⁺). Note that in the presence of calcium the upper band of the doublet (intact myosin VI) preferentially binds to liposomes. **(c)** The lipid-binding site is within amino acids 1077–1133 of the myosin VI C-terminal tail. The percentage total protein in pellet fractions after sedimentation with mixed brain liposomes were measured by quantification of SDS–PAGE gels. Each binding experiment was repeated at least three times and a typical experiment is shown. Tail fragments tested were: N-terminal tail without or with the large insert (NT, amino acids 845–1032; NT + LI, amino acids 845–1060); the C-terminal tail without the large insert (CT amino acids 1077–1276); the ΔPtdInsP₂ tail (amino acids

845–1276 with residues 1059–1134 deleted); and the following mutations in CT: RRL→AAA, WWY→WLY, WKSKNKKR→WASANNNR (amino acids 1115–1122), the last 142 amino acids of the C-terminal tail (CT 1134–1276), and the 11K tryptic digest fragment (domain 2). **(d)** SDS–PAGE (15% acrylamide) gel showing C-terminal myosin VI tail (CT) and tryptic digests of the C-terminal tail in the absence and presence of liposomes. Digestion without liposomes results in cleavage at site 1 (see Supplementary Information, Fig. S1b) and yields two fragments (18K and 11K: labelled 1 and 2, respectively), whereas digestion in the presence of liposomes leads to cleavage at site 2 (see Supplementary Information, Fig. S1b) and new fragments (fragment 3 is indicated). **(e)** Domain 2 in the C-terminal tail of myosin VI contains the lipid binding site. The tryptic digest of the C-terminal tail (in the absence of liposomes as in **d**) was incubated with liposomes and centrifuged. Both undigested C-terminal tail and domain 2 are in the pellet fraction, indicating that they bind to liposomes.

it is likely that calcium must have some effect on the conformation of the whole molecule — probably binding to the calmodulin molecules in the neck/linker region in the motor domain. Frequently, full-length myosin VI preparations expressed and purified from baculovirus and/or insect cells migrate as a closely spaced doublet on SDS–PAGE (Fig. 2b) and over time the top band decreases and the bottom band increases, most likely reflecting proteolysis. As the N-terminus of the myosin VI molecule with its His-tag is still intact, proteolysis must occur at the extremely sensitive tryptic cleavage site (R1122) identified near the lipid-binding region in the C-terminal tail domain (see Supplementary Information, Fig. S1b). This proposal is supported by the observation that more of the top (intact) myosin VI band (90%) is bound to liposomes compared with the lower band (40%) in the sedimentation assays (Fig. 2b) and this is consistent with the lipid binding site being localized to this region of the C-terminal tail.

To determine whether myosin VI exhibits specificity for different phosphoinositides, lipid binding to the C-terminal tail was tested using liposomes containing 10% of the series of phosphoinositides

shown in Fig. 3a. The C-terminal tail binds with high specificity to PtdIns(4,5)P₂-containing liposomes, and exhibits little or no binding to the other phosphoinositides (Fig. 3a). To establish the concentration of PtdIns(4,5)P₂ necessary for liposome binding to myosin VI, synthetic liposomes were prepared with a range of PtdIns(4,5)P₂ concentrations. The minimal concentration of PtdIns(4,5)P₂ in the synthetic liposomes required for myosin VI binding was approximately 2–5% (Fig. 3b). Liposomes prepared from mixed brain lipids (“folch” fraction I) contain a minimum of 10% PtdIns(4,5)P₂ and exhibit the strongest binding to the myosin VI tail. The strength of lipid binding was determined by fluorescence resonance energy transfer (FRET) between tryptophan groups on the myosin VI tail and dansyl-labelled PtdIns(4,5)P₂-containing liposomes (Fig. 3c). Addition of increasing amounts of tail protein to a fixed amount of liposomes results in a hyperbolic curve, indicating that the binding is non-cooperative (Fig. 3c). A K_d of 0.3 μM was measured indicating that the C-terminal tail region binds strongly to PtdIns(4,5)P₂ liposomes.

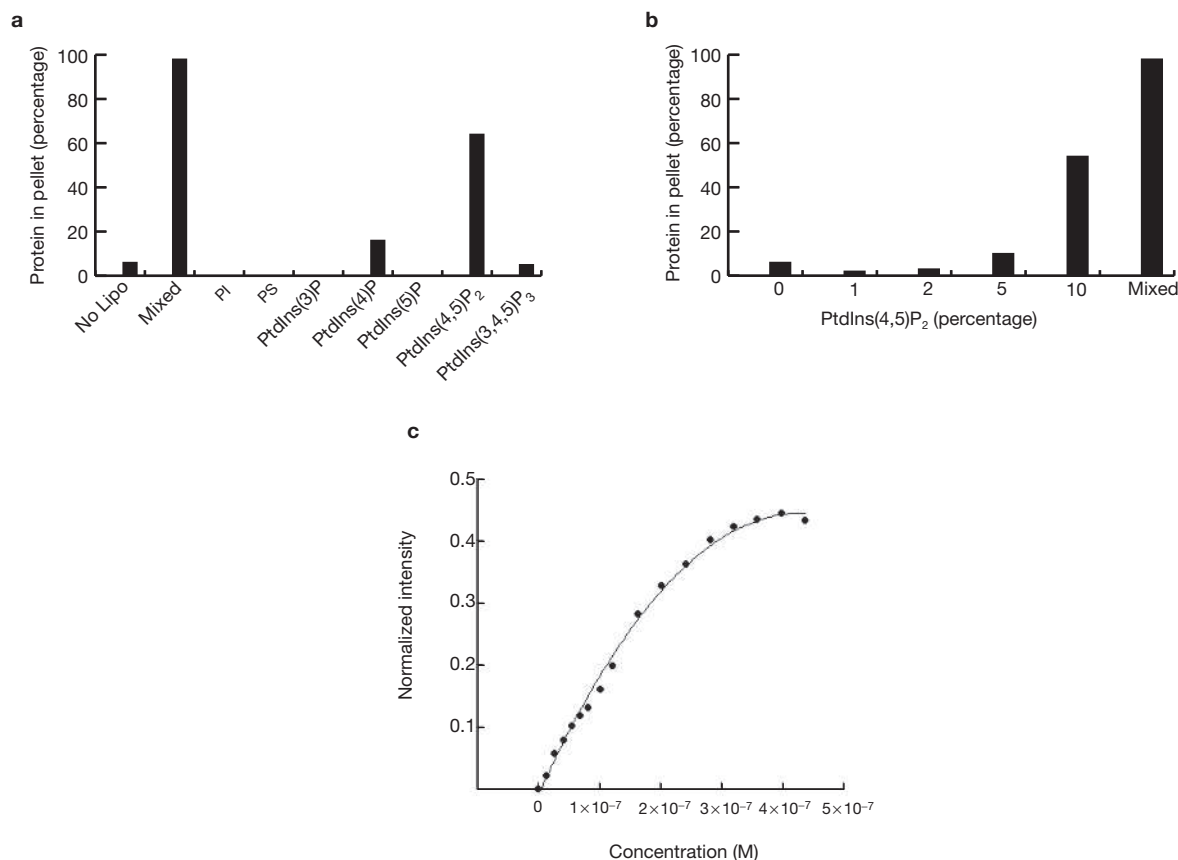


Figure 3 Myosin VI binds specifically to PtdIns(4,5)P₂-containing liposomes. **(a)** The binding of the myosin VI C-terminal tail was tested with liposomes of varying compositions (liposomes contained 40% phosphatidylcholine (PC), 40% phosphatidylethanolamine (PE), 10% cholesterol and 10% of a variable phosphoinositide), and the percentage of protein in the pellet after sedimentation was measured as in Fig. 2c. The binding experiments were repeated three times and a typical experiment where the percentage binding relative to the binding to mixed brain liposomes (100%) is shown. The tail binds strongly to PtdIns(4,5)P₂-containing liposomes and to mixed brain liposomes (Folch fraction I), whereas no or little binding was observed to liposomes containing PI (phosphatidylinositol), PS (phosphatidylserine),

PtdIns(3)P, PtdIns(4)P, PtdIns(5)P or PtdIns(3,4,5)P₃. **(b)** The C-terminal tail was tested against liposomes containing 10% cholesterol, 40% phosphatidylcholine and 40% phosphatidylethanolamine and varying amounts of PtdIns(4,5)P₂ using the sedimentation assay in Fig. 2c. A minimum of 2–5% PtdIns(4,5)P₂ was required for binding, although maximal binding was seen using mixed liposomes that contain a minimum of 10% PtdIns(4,5)P₂. **(c)** FRET between tryptophan groups on the C-terminal tail and dansylated liposomes (composed of 10% cholesterol, 10% PtdIns(4,5)P₂, 40% phosphatidylcholine and 40% dansylated phosphatidylethanolamine) was measured and the resulting curve was fit using Kaleidograph to obtain the K_d (0.3 μ M).

To investigate whether lipid binding had any effect on the secondary structure of the C-terminal myosin VI tail, its circular dichroic spectrum was measured with and without liposomes. The circular dichroic spectrum of the C-terminal tail alone indicates a protein with a mixed secondary structure composition (Fig. 4a). However, with liposomes, the circular dichroic spectrum altered to that of an α -helical protein (with double minima at 208 and 222 nm) within 5 min (Fig. 4a). The α -helical signal (ellipticity at wavelength 222 nm) increased by 31% on addition of liposomes, indicating that lipid binding induces significant α -helix formation in the C-terminal region of the myosin VI tail. The liposomes themselves showed no circular dichroic signal in the range of wavelength used (200–250 nm) and, as expected, there was no significant change in the circular dichroic spectra of the N-terminal tail region with liposomes (Fig. 4a).

As the microtubule-based kinesin motor KIF1A (also known as Unc104) seems to dimerize on lipid binding¹², we tested whether liposome binding induces dimerization of the myosin VI C-terminal tail by using the zero-length crosslinker 1-ethyl-3-(3-dimethylaminopropyl) carbodiimide (EDC). Without liposomes, the C-terminal tail is still a

monomer on SDS–PAGE after incubation with EDC for 1 h (Fig. 4b, c), in agreement with our previous data using full-length expressed or native myosin VI (ref. 13). However, after incubation with EDC in the presence of increasing amounts of liposomes, an obvious dimer band and then tetramer and higher-order multimers were detected (Fig. 4b, c). To determine the minimal concentration of EDC crosslinker required for dimerisation, C-terminal tail with liposomes was incubated with increasing amounts of EDC. Using 0.1–2 mM EDC only monomer bands were observed, whereas at 10 mM EDC the monomer band decreased and a faint dimer band began to emerge. On addition of 20 mM EDC, a stronger dimer band was visible (Fig. 4d). Precisely how the C-terminal tail is crosslinked on the surface of the liposomes is unclear as it does not contain any predicted coiled-coil regions or other recognizable dimerization motifs (see Supplementary Information, Fig. S1b). Whether myosin VI attached to lipid vesicles functions in the cell as monomers, dimers, or even as multimers, is still unresolved.

To investigate the role of PtdIns(4,5)P₂-lipid binding on the *in vivo* functions of myosin VI, we expressed GFP-labelled full-length myosin VI and tail, and the corresponding mutants containing PtdIns(4,5)P₂

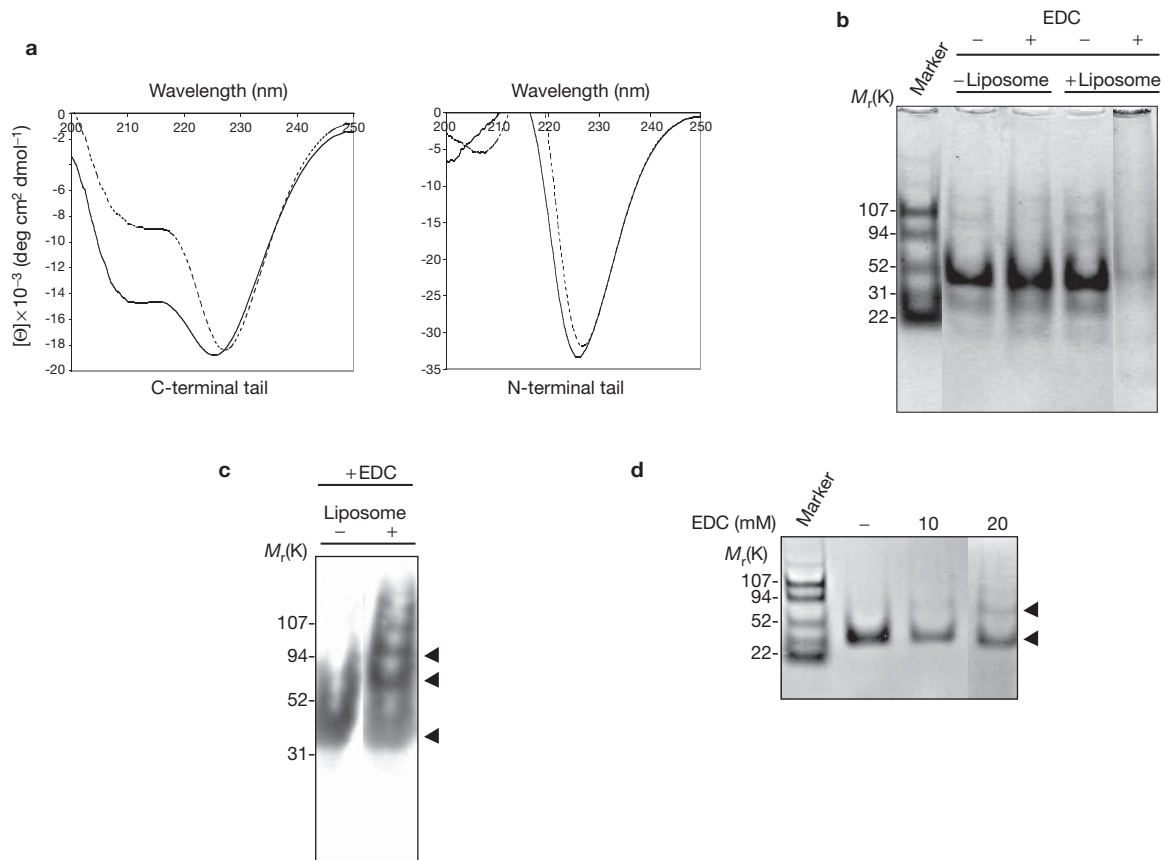


Figure 4 Liposome binding increases the helical structure of the C-terminal tail of myosin VI and induces dimerization. **(a)** Circular dichroic spectra of the myosin VI C-terminal tail and the N-terminal tail with (solid lines: + 0.2 mg ml⁻¹ liposomes) or without mixed brain liposomes (dashed lines). An average of five spectra are shown, normalized against spectra of buffer alone or buffer + liposomes. With liposomes, the C-terminal tail adopts a highly helical spectrum and the (helical) signal at 222 nm increases by 31%, whereas the spectrum of the N-terminal tail is not altered (this construct does not bind liposomes in sedimentation assays: see Fig. 2c). **(b)** Liposome binding induces multimerization of the myosin VI C-terminal tail. C-terminal tail (12 μM) was incubated with or without 0.4 mg ml⁻¹ mixed brain liposomes and/or 90 mM EDC, a zero-length crosslinker, and analysed by SDS-PAGE. Without liposomes the monomer

C-terminal tail (30K) is not crosslinked by EDC, but with both liposomes and EDC, the monomer band multimerizes and remains at the top of the gel. BSA was used as a negative control and was not crosslinked on addition of liposomes and EDC (data not shown). **(c)** Western blot of the C-terminal tail (+/- liposomes, + 90 mM EDC) using a polyclonal myosin VI C-terminal antibody. Without liposomes, only a monomer band is visible, whereas with liposomes, dimer, tetramer (indicated by the arrows) and trace higher-order bands can be detected. **(d)** Liposome binding induces dimerization of the myosin VI C-terminal tail. The SDS-PAGE gel shows C-terminal tail (12 μM) after a 1 h incubation with 0.4 mg ml⁻¹ mixed brain liposomes and no EDC, 10 mM EDC, 20 mM EDC. The positions of monomer and dimer bands are indicated with black arrowheads. Bio-Rad prestained SDS-PAGE markers are also shown.

binding-site mutations (WASANNR). Both the full-length myosin VI and tail with the PtdIns(4,5)P₂ binding-site mutations showed considerably less recruitment to CCSs compared with their wild-type constructs (Fig. 5a). Quantification of the immunofluorescence images showed that mutation of the PtdIns(4,5)P₂ binding site reduces the recruitment of both full-length myosin VI and its tail domain by approximately 50% (Fig. 5b). As an alternative approach to quantify the localization of myosin VI to CCSs, GFP-labelled wild-type myosin VI tail and the GFP-labelled mutant tail missing the PtdIns(4,5)P₂ binding region (Δ PtdIns(4,5)P₂ tail) were expressed and the GFP-tail constructs were immunoprecipitated using GFP antibodies to pull down the tail-clathrin complexes. Although slightly higher levels of the mutant tail are expressed in the cells, far less clathrin is associated with the Δ PtdIns(4,5)P₂ tail compared with the wild-type tail (Fig. 5c). Thus, the targeting and functional role of full-length myosin VI in CCSs in the early endocytic pathway is mediated by the C-terminal domain binding to both Dab2 and PtdIns(4,5)P₂ and requires the presence of the large insert in the tail domain.

We have demonstrated that the C-terminal tail of myosin VI is composed of two key domains that contain 'hot spots' for binding adaptor proteins — the WWY (1183–1185) and RRL (1107–1110) sites and a PtdIns(4,5)P₂ lipid-binding region that are crucial for targeting and/or recruiting myosin VI to distinct compartments within the cell. Previous coimmunoprecipitation studies indicated that the binding between the myosin VI tail and its adaptor proteins was relatively weak⁴. Low affinity protein-protein interactions, as observed in many clathrin and AP-2 binding proteins^{14,15}, are essential for the rapid and accurate coordination between the vast range of components involved in membrane trafficking pathways, such as endocytosis. The hydrophobic Dab2-binding site (WWY) is in an extensive region in the myosin VI tail that is predicted to be unstructured by multiple secondary structure prediction algorithms (performed using the NPS@Network Protein Sequence Analysis web server¹⁶; see Supplementary Information, Fig. S1b). These unfolded regions are believed to have important roles in many endocytic proteins^{14,17,18}; for example, it has been suggested that these unfolded regions

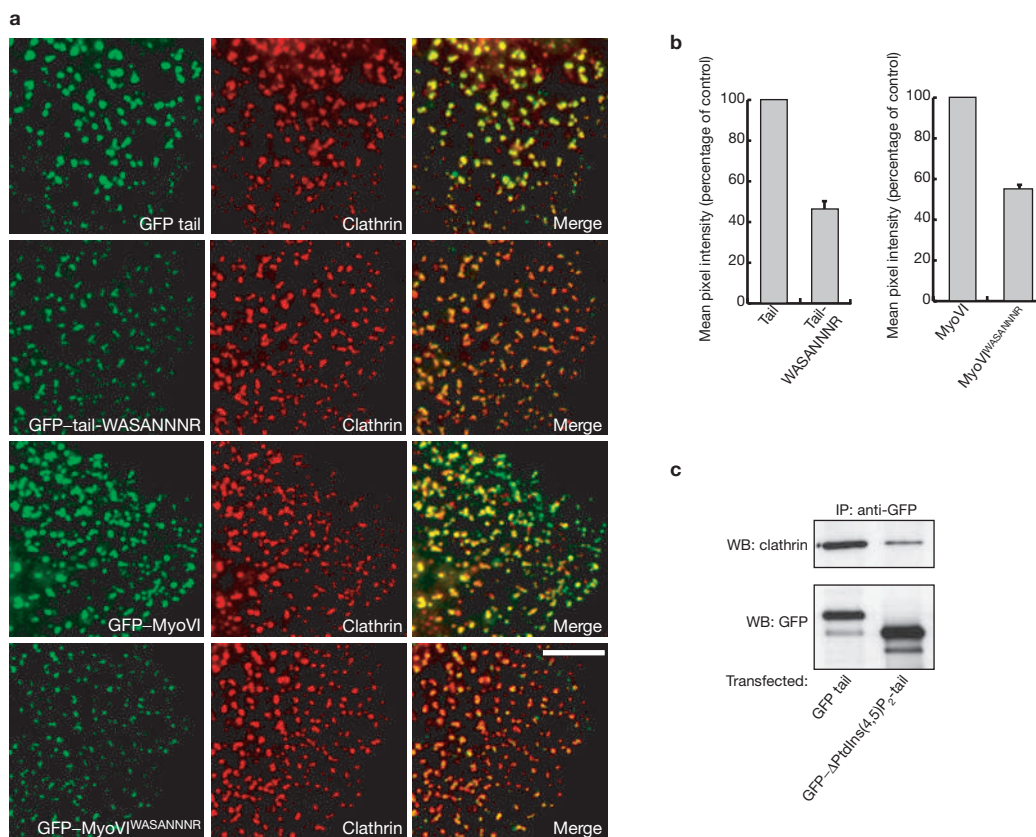


Figure 5 Mutations in the PtdIns(4,5) P_2 binding site reduce the targeting of myosin VI to clathrin-coated structures *in vivo*. **(a)** HeLa cells were transfected with full-length wild-type GFP-myosin VI or GFP-tail or mutants containing the WASANNR point mutation in the PtdIns(4,5) P_2 binding site, as indicated, and processed for immunofluorescence microscopy with anti-GFP and anti-clathrin antibodies. Both tail domain and full-length myosin VI with mutations in the PtdIns(4,5) P_2 binding site show significantly reduced recruitment to clathrin-coated structures at the plasma membrane. The fluorescence intensity of the different GFP-labelled constructs in at least 500 individual CCSs was measured using IP-Lab software. The scale bar represents 5 μ m. **(b)** The bar graphs show the mean pixel intensity of

GFP fluorescence on CCSs of the mutant constructs relative to the wild-type controls. The results shown are the mean values of two independent experiments (\pm s.e.m.). **(c)** In a separate experiment, HeLa cells were transfected with intact GFP-tagged myosin VI tail or GFP-tails with a 75 amino acid deletion of the PtdIns(4,5) P_2 binding region (Δ PtdIns(4,5) P_2 -tail) and the expressed GFP-proteins were immunoprecipitated with anti-GFP antibodies. The immunoprecipitated (IP) complexes were run on SDS-PAGE and blotted with antibodies against clathrin. One fifth of each of the immunoprecipitated samples were run on the same gel and blotted with GFP antibodies to ensure that equal overexpression and immunoprecipitation of both tail constructs had occurred.

contain binding sites that act as a flexible 'string to fish for and hook' binding partners and, on binding, these unstructured regions may become structured¹⁴. The large increase in helicity (31%) in the myosin VI tail when it binds PtdIns(4,5) P_2 would fit in with this model. The observation that the C-terminal tail region of myosin VI contains a flexible, proteolytically susceptible, linker region connecting two functional domains (see Supplementary Information, Fig. S2) provides further support for such a model. PtdIns(4,5) P_2 is a crucial second messenger^{19,20} that is known to bind and recruit many endocytic proteins to the plasma membrane^{21,22} and regulate the formation, scission and uncoating of clathrin-coated vesicles. Thus, myosin VI, by binding not only to Dab2 but also to PtdIns(4,5) P_2 concentrated in the plasma membrane at active sites of endocytosis, may be recruited to the membrane at a very early stage of clathrin-coated pit assembly (see Supplementary Information, Fig. S2). The region in the myosin VI tail that binds PtdIns(4,5) P_2 contains a motif of basic residues (R/K) alternating with hydrophobic residues that is very similar to the region identified in a number of cytoskeletal proteins that have been shown to bind to PtdIns(4,5) P_2 (ref. 23). The monomeric kinesin motor KIF1A dimerizes on liposome binding and the resulting dimer can

transport the liposome processively along microtubules²⁴. It is possible that such a scenario could occur with monomeric myosin VI (ref. 13); that is, could it dimerize on liposome binding and then work as a processive motor? The most recent *in vitro* results on the functional state of myosin VI are intriguing but contradictory. Full-length myosin VI monomers can be induced to form a few processive dimers (17%) when clustered on actin filaments²⁵. On the other hand, a single myosin VI monomer, when coupled to a polystyrene bead of a similar size to an intracellular vesicle, can move processively with a large step (40 nm)²⁶. Thus, whether myosin VI exists and functions in the cell as a monomer and/or dimer remains to be established. However, if myosin VI has a major role in vesicular trafficking, then its dimerization on the surface of a lipid vesicle to generate a processive motor would be an efficient mechanism for regulating this transport function. One of our next major challenges is to establish how the protein-binding partners, inserts and PtdIns(4,5) P_2 affect the structure, properties and functional (monomer-dimer-multimer) state of myosin VI and determine its role(s) *in vivo* in membrane-trafficking pathways, such as clathrin-mediated endocytosis (see Supplementary Information, Fig. S2). □

METHODS

Human myosin VI isoforms and antibodies. The human myosin VI (+ large insert) was generated from KIAA 0389 clone from Human cDNA Bank Section, (Kazusa DNA Research Institute, Chiba, Japan) and cloned into the pEGFP-C3 vector for mammalian transient expression. Intact chicken myosin VI (+large insert) was expressed in Sf9 insect cells using the Baculovirus expression system and purified and checked for activity as previously described¹³. Mouse monoclonal anti-clathrin X-22 and rabbit polyclonal anti-GFP antibodies were from AbCam (Cambridge, UK) and the rabbit polyclonal myosin VI tail antibody as previously described². Rabbit anti-clathrin heavy chain antibody used for the western blot was from M.S. Robinson (CIMR, Cambridge, UK).

Cell culture, transfection, immunofluorescence microscopy and immunoblotting. HeLa cells grown on coverslips to 50% confluency were transfected using FuGENE (Roche Diagnostics, Lewes, UK) overnight with 2 µg of intact human myosin VI (+large insert) or only the tail domain in pEGFP vector. To visualize myosin VI associated with clathrin-coated or uncoated vesicles, cells were permeabilized with 0.05% saponin in PBS for 30 s before fixing with paraformaldehyde. Cells were visualised in a Zeiss Axioplan microscope and data analysed with IP-Lab software (Zeiss, Welwyn, UK). Colocalization of GFP-myosin VI with clathrin was quantified in the cell periphery of GFP-myosin VI transfected cells double-labelled for clathrin. On average 50 CCSs were counted in at least 5–10 cells for each construct. In the quantitative immunostaining experiments identical acquisition settings were used and circles were manually drawn around single CCSs and the mean pixel intensity was determined for the region of interest. At least 500 CCSs were measured for each construct (20–30 CCSs per cell and at least ten cells per experiment) and the experiment was repeated twice. The measurements were normalized for the intensity of clathrin staining in each sample. Immunoprecipitation assays using GFP antibodies to pulldown GFP-myosin VI tail-clathrin complexes were carried out as previously described²⁷.

Identification of Dab2 and GIPC binding sites. Chicken brush-border myosin VI intact tail (+LI; amino acids 840–1277) was used as a template to generate a series of myosin VI tail deletion mutants by PCR. To narrow down the binding sites in the tail, alanine scanning mutations (mutating three consecutive residues at a time to Ala) and binding-site mutations were generated by PCR using the QuikChange Site-Directed Mutagenesis kit (Stratagene, Amsterdam, The Netherlands). All these tail mutants were cloned into the pM 'bait' vector, whereas binding partners (Dab2, GIPC, and optineurin) were cloned into the pV16 'prey' vector (Clontech, Saint Germain-en-Laye, France) and the mammalian two-hybrid assay was performed in CHO cells as previously described⁷. For the pulldown assays, GST-tagged chicken myosin VI intact tail (+LI; wild type or W1184L or RRL->AAA mutants) were expressed in *Escherichia coli* and purified as previously described²⁷. Full-length Dab2 was cloned into pcDNA3 (Invitrogen, Paisley, UK), *in vitro* translated and labelled with ³⁵S-methionine using the TNT-coupled Reticulocyte Lysate system (Promega, Southampton, UK). The pulldown assays were performed as previously described⁴.

Expression, purification and digestion of myosin VI tail constructs. Chicken myosin VI intact tail (+LI) constructs were generated by PCR and mutants prepared using the QuikChange Site-Directed Mutagenesis kit (Stratagene). The tail fragments were cloned into the pRSET vector, expressed in *E. coli* C41 cells and purified essentially as described previously²⁷ with the following modifications: soluble C-terminal tail fragments, after cell lysis, were first passed over an anion exchange matrix (Whatman DE53, Brentford, UK) and then applied to a Ni-NTA column (Qiagen, Crawley, UK), washed and His-tagged tail fragments eluted with TBS + 300 mM imidazole at pH 7.4. Insoluble full-length chicken myosin VI tail constructs were dissolved in 8 M urea, 10 mM Tris-HCl at pH 8.0, 100 mM NaCl, 1 mM DTT before applying to the DE-53 resin. The flow-through was applied to the Ni-NTA column, washed with 8 M urea in TBS, and the protein was refolded on the column by stepwise washes (4 M urea, 2 M urea, no urea in TBS) before elution with TBS + 300 mM imidazole at pH 7.4. The proteins were dialysed and diluted with HEPES-salt solution (20 mM HEPES at pH 7.4, 150 mM NaCl, 1 mM DTT). The C-terminal myosin VI tail domain (14 µM) in HEPES-salt solution without and with (0.4 mg ml⁻¹) liposomes was digested with trypsin (type T1426; Sigma, Gillingham, UK) for 30 min at 0 °C (protein to trypsin molar ratio of 500:1). Digestion was stopped by the addition of a twofold

molar excess of trypsin inhibitor (Sigma type T0256). The resulting fragments were electroblotted onto Immobilon-PVDF membrane (Millipore, Watford, UK) and their N-terminal sequences determined using an Applied Biosystems Procise 494 Sequencer and further analysed using MALDI-TOF mass spectrometry. As the 11K domain 2 retains the His tag, it can be separated from 18K domain 1 by chromatography on a Ni-NTA column in HEPES-salt solution (non-dissociating conditions) as described above.

Lipid-binding assay. Mixed brain liposomes (Folch fraction 1, Sigma B1502) and liposomes made from 40% phosphatidylcholine, 40% phosphatidylethanolamine, 10% cholesterol and 10% of a variable phosphoinositol (excluding PtdIns(4,5)P₂) obtained from Avanti Polar Lipids (Delfzijl, The Netherlands) were treated with chloroform, aspirated under argon and then dried under vacuum for 10 min before resuspension by sonication in 20 mM HEPES at pH 7.4, 150 mM NaCl and 1 mM DTT to a final concentration of 1 mg ml⁻¹ (ref. 28). Protein (4 µM) and 0.4 mg ml⁻¹ liposomes were mixed, incubated and centrifuged for 15 min at 160,000g at 4 °C. Supernatant and pellet fractions were analysed on SDS-PAGE (10 or 15% acrylamide) gels using prestained high- or broad-range standards (Biorad, Hemel Hempstead, UK) for calibration. Gels were analysed using a Molecular Dynamics densitometer and ImageQuant software (the intensity of the tail band in the pellet was divided by the total intensity (pellet + supernatant) for each sample to determine the percent of protein in the pellet).

Fluorescence resonance energy transfer. A Perkin Elmer (Beaconsfield, UK) LS55 luminescence spectrometer was used to measure FRET between tryptophan groups on the myosin VI C-terminal tail and dansylated liposomes consisting of 10% cholesterol, 10% PtdIns(4,5)P₂, 40% phosphatidylcholine and 40% Dansyl-phosphatidylethanolamine (Avanti Polar Lipids). 11 µM Protein (11 µM) was titrated into 16 µg ml⁻¹ liposomes in buffer (20 mM HEPES, 150 mM NaCl, 1 mM DTT) at constant temperature (20 °C) using a Hamilton Microlab 500 syringe pump. An excitation of 340 nm was used, and the emission intensity at 520 nm (I) was normalized against the intensity without addition of protein (I₀), resulting in (I-I₀)/I₀, which was plotted against protein concentration. Kaleidograph was used to obtain the K_d from the following curve-fit: $I_{\text{max}} = (I - I_0) / I_0 / K_d + (I - I_0) / I_0 + c$ where I_{max} is maximum intensity, K_d is the binding constant, and c is a constant. The measured K_d was 0.3 µM, or 1.4 µM on incorporation of a linear decay in the curve fit. The non-binding tail fragment (1134–1276) was used as a control.

Circular dichroism and crosslinking experiments. Five spectra for each protein (8–14 µM in 20 mM HEPES at pH 7.4, 150 mM NaCl, 1 mM DTT) at 20 °C were measured and averaged on a Jobin Yvon CD6 spectrometer with the spectrum of salt and buffer alone subtracted. 50 µl of 1 mg ml⁻¹ mixed brain liposomes (in above HEPES-salt solution) were added to 200 µl of the protein sample and the spectra were measured immediately.

The zero length crosslinker EDC (Sigma, E-1769; final concentrations 20–90 µM) was added to 50 µl aliquots of myosin VI C-terminal tail (12 µM) in HEPES-salt solution alone or after addition of 0.4 mg ml⁻¹ mixed brain liposomes. After incubation at room temperature for 1 h, a phosphate loading buffer (pH 6.2) was added (25 mM NaH₂PO₄, 37 mM Na₂HPO₄, 3.5 mM SDS, 10% β-mercaptoethanol, 10% glycerol, 4 M urea, 0.01% bromophenol blue) and samples were analysed by SDS-PAGE using phosphate buffered gels (25 mM NaH₂PO₄, 72 mM Na₂HPO₄, pH 7.4, 3.5 mM SDS, 4.5% acrylamide) and phosphate running buffer (25 mM NaH₂PO₄, 72 mM Na₂HPO₄, 3.5 mM SDS, pH 7.4). Crosslinked phosphorylase-b molecular weight marker (Sigma) was used to calibrate the gels.

Note: Supplementary Information is available on the Nature Cell Biology website.

ACKNOWLEDGEMENTS

We thank: B. Peter and H. McMahon for help with lipid binding assays and discussion; R. Williams, D. Veprintsev and O. Perisic for programmes and help with the FRET assay; S. Peak-Chew and F. Begum for N-terminal sequencing and mass spectrometry; and D. Owen for critical reading of the manuscript. The work was funded by a USA Royal Society Postdoctoral Fellowship (G.S.), a Croucher Foundation (Hong Kong) Student Scholarship (J.S.A.), a Wellcome Trust Senior Fellowship (F.B.) and was supported by the Medical Research Council. The Cambridge Institute for Medical Research is in receipt of a strategic award from the Wellcome Trust.

AUTHOR CONTRIBUTIONS

Each of the authors made a significant contribution to the experimental work described.

COMPETING FINANCIAL INTERESTS

The authors declare that they have no competing financial interests.

Published online at <http://www.nature.com/naturecellbiology/>

Reprints and permissions information is available online at <http://npg.nature.com/reprintsandpermissions/>

- Wells, A. L. *et al.* Myosin VI is an actin-based motor that moves backwards. *Nature* **401**, 505–508 (1999).
- Buss, F., Arden, S. D., Lindsay, M., Luzio, J. P. & Kendrick-Jones, J. Myosin VI isoform localized to clathrin-coated vesicles with a role in clathrin-mediated endocytosis. *EMBO J.* **20**, 3676–3684 (2001).
- Aschenbrenner, L., Lee, T. & Hasson, T. Myo6 facilitates the translocation of endocytic vesicles from cell peripheries. *Mol. Biol. Cell* **14**, 2728–2743 (2003).
- Sahlender, D. A. *et al.* Optineurin links myosin VI to the Golgi complex and is involved in Golgi organization and exocytosis. *J. Cell Biol.* **169**, 285–295 (2005).
- Warner, C. L. *et al.* Loss of myosin VI reduces secretion and the size of the Golgi in fibroblasts from Snell's waltzer mice. *EMBO J.* **22**, 569–579 (2003).
- Geisbrecht, E. R. & Montell, D. J. Myosin VI is required for E-cadherin-mediated border cell migration. *Nature Cell Biol.* **4**, 616–620 (2002).
- Morris, S. M. *et al.* Myosin VI binds to and localises with Dab2, potentially linking receptor-mediated endocytosis and the actin cytoskeleton. *Traffic* **3**, 331–341 (2002).
- Dance, A. L. *et al.* Regulation of myosin-VI targeting to endocytic compartments. *Traffic* **5**, 798–813 (2004).
- Bunn, R. C., Jensen, M. A. & Reed, B. C. Protein interactions with the glucose transporter binding protein GLUT1CBP that provide a link between GLUT1 and the cytoskeleton. *Mol. Biol. Cell* **10**, 819–832 (1999).
- Lou, X., McQuistan, T., Orlando, R. A. & Farquhar, M. G. GAIP, GIPC and Gai3 are concentrated in endocytic compartments of proximal tubule cells: putative role in regulating megalin's function. *J. Am. Soc. Nephrol.* **13**, 918–927 (2002).
- Pashkova, N., Jin, Y., Ramaswamy, S. & Weisman, L. S. Structural basis for myosin VI discrimination between distinct cargoes. *EMBO J.* **25**, 693–700 (2006).
- Klopfenstein, D. R., Tomishige, M., Stuurman, N. & Vale, R. D. Role of phosphatidylinositol(4,5)bisphosphate organization in membrane transport by the Unc104 kinesin motor. *Cell* **109**, 347–358 (2002).
- Lister, I. *et al.* A monomeric myosin VI with a large working stroke. *EMBO J.* **23**, 1729–1738 (2004).
- Evans, P. R. & Owen, D. J. Endocytosis and vesicle trafficking. *Curr. Opin. Struct. Biol.* **12**, 814–821 (2002).
- Dell'Angelica, E. C. Clathrin-binding proteins: got a motif? Join the network! *Trends Cell Biol.* **11**, 315–318 (2001).
- Combet, C., Blanchet, C., Geourjon, C. & Deleage, G. NPS@: network protein sequence analysis. *Trends Biochem. Sci.* **25**, 147–150 (2000).
- Brett, T. J., Traub, L. M. & Fremont, D. H. Accessory protein recruitment motifs in clathrin-mediated endocytosis. *Structure (Camb)* **10**, 797–809 (2002).
- Kalthoff, C., Alves, J., Urbanke, C., Knorr, R. & Ungewickell, E. J. Unusual structural organization of the endocytic proteins AP180 and epsin 1. *J. Biol. Chem.* **277**, 8209–8216 (2002).
- Sakisaka, T., Itoh, T., Miura, K. & Takenawa, T. Phosphatidylinositol 4,5-bisphosphate phosphatase regulates the rearrangement of actin filaments. *Mol. Cell Biol.* **17**, 3841–3849 (1997).
- Czech, M. P. PIP2 and PIP3: complex roles at the cell surface. *Cell* **100**, 603–606 (2000).
- Cremona, O. & De Camilli, P. Phosphoinositides in membrane traffic at the synapse. *J. Cell. Sci.* **114**, 1041–1052 (2001).
- Itoh, T. & Takenawa, T. Regulation of endocytosis by phosphatidylinositol 4,5-bisphosphate and ENTH proteins. *Curr. Top. Microbiol. Immunol.* **282**, 31–47 (2004).
- Janmey, P. A., Xian, W. & Flanagan, L. A. Controlling cytoskeleton structure by phosphoinositide-protein interactions: phosphoinositide binding protein domains and effects of lipid packing. *Chem. Phys. Lipids* **101**, 93–107 (1999).
- Klopfenstein, D. R. & Vale, R. D. The lipid binding pleckstrin homology domain in UNC-104 kinesin is necessary for synaptic vesicle transport in *Caenorhabditis elegans*. *Mol. Biol. Cell.* **15**, 3729–3739 (2004).
- Park, H. *et al.* Full-length myosin VI dimerizes and moves processively along actin filaments upon monomer clustering. *Mol. Cell* **21**, 331–336 (2006).
- Iwaki, M. *et al.* Cargo binding makes a wild-type single-headed myosin-VI move processively. *Biophys J.* **90**, 3643–3652 (2006).
- Buss, F. *et al.* The localization of myosin VI at the Golgi complex and leading edge of fibroblasts and its phosphorylation and recruitment into membrane ruffles of A431 cells after growth factor stimulation. *J. Cell Biol.* **143**, 1535–1545 (1998).
- Peter, B. J. *et al.* BAR domains as sensors of membrane curvature: the amphiphysin BAR structure. *Science* **303**, 495–9 (2003).

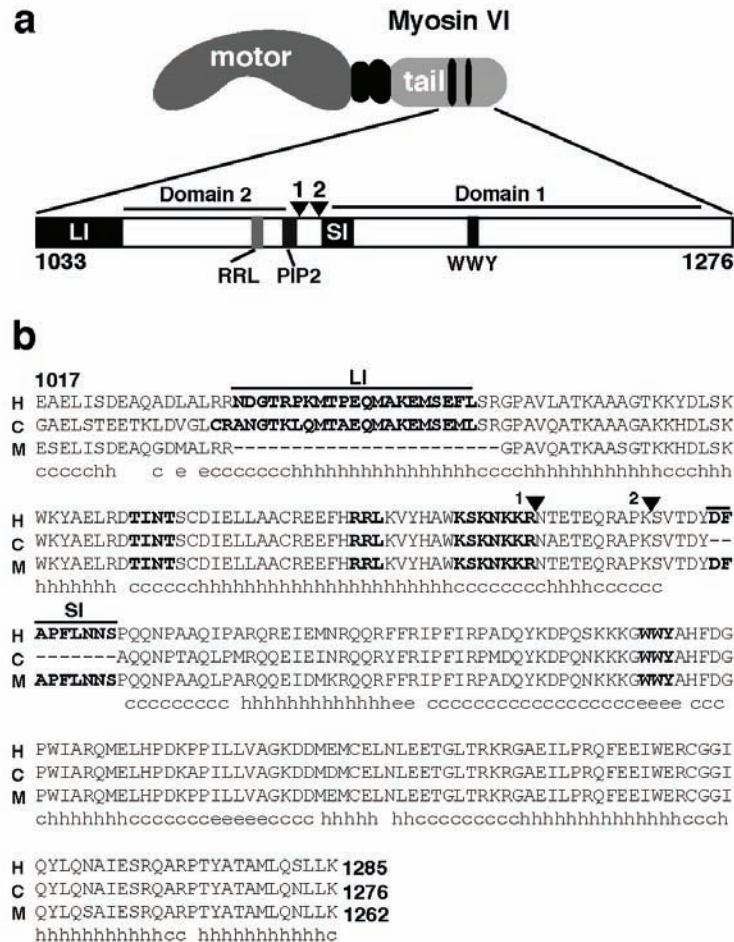


Figure S1 A cartoon showing the domain organisation of full-length myosin VI and a schematic and sequence alignment of C-terminal region of the tail. **(a)** The cartoon depicts the domain organisation of myosin VI highlighting the globular C-terminal tail with the relative positions of the splice inserts (LI: large insert, SI: small insert), the binding sites for Dab2 and GIPC/optineurin [positions 1184aa (W) and 1107-1109aa (RRL) respectively] and the PIP₂ binding site. Black arrowheads (1 and 2) indicate the tryptic cleavage sites and black lines show the positions of domains 1 and 2. The amino acid (aa) numbering refers to the

chicken sequence. **(b)** An alignment of the human (H), chicken (C) and mouse (M) myosin VI C-terminal tail sequences (aa 1017 – end) using ClustalW from www.ch.EMBLnet.org. The large and small inserts (LI and SI) and the RRL, WWY, and lipid (KSKNKKR) binding sites are shown in bold along with the phosphorylatable TINT sequence¹. Arrowheads 1 and 2 mark the trypsin cleavage sites. Predicted secondary structure for the chicken myosin sequence obtained by a consensus of 8 prediction algorithms² is shown: “c” is random coil, “e” is extended sheet, “h” is α helix and a blank space indicates no consensus.

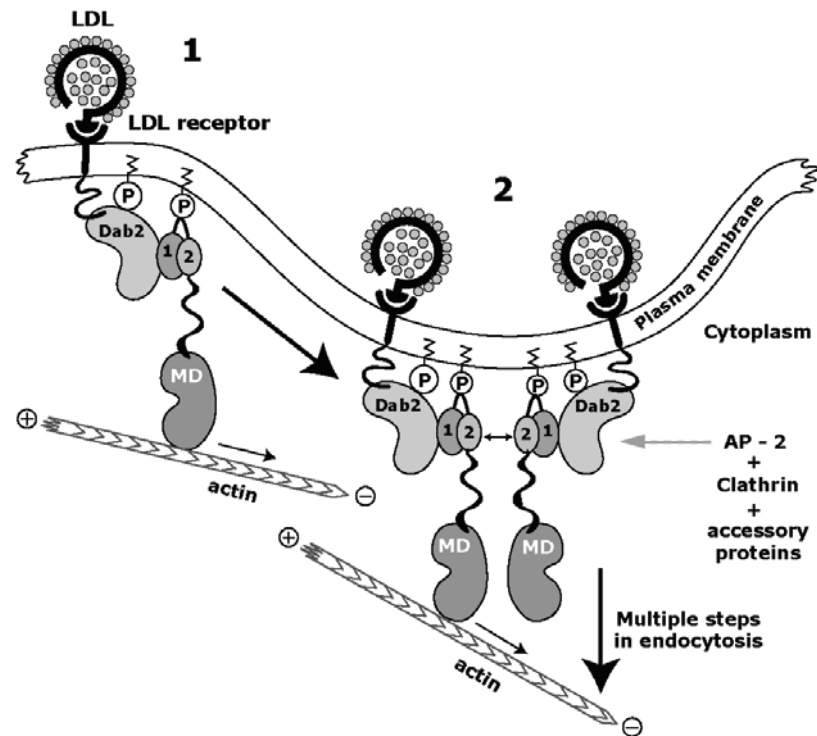


Figure S2 Possible roles for myosin VI in the early stages of clathrin mediated endocytosis. We speculate that at (1) Dab2 is bound via its N-terminal phosphotyrosine (PTB) motif to the cytoplasmic tail of a LDL receptor³ and is bound to PIP₂ (P) in the plasma membrane⁴. Myosin VI (MD denotes its motor domain and 1 and 2 the domains in the C-terminal tail) is recruited to the plasma membrane by binding to Dab2 and also to PIP₂ (P). Possibly by interacting with newly polymerised actin filaments (initiated by the WASP/Scar/PIP₂ and Arp2/3 complexes⁵), myosin VI could cluster the receptors and then generate sufficient force to pull the membrane inwards to form a nascent clathrin coated

pit at (2). The clustering of myosin VI in such a 'pit' might favour dimerisation or multimerisation (possible CT tail interactions indicated by double headed arrow) and the resulting myosin VI dimers (multimers) together with the endocytic machinery (AP-2, clathrin and accessory proteins) and the actin filament network could be involved in the formation of clathrin coated vesicles, their uncoating and then subsequent delivery into the cell. At this stage it should be stressed that multiple myosin VI monomers might also be able to accomplish the same tasks. A recent relevant review by Lois Weisman⁶ explores possible molecular mechanisms for membrane-cargo transport by myosin V.

Supplementary references

1. Sahlender, D.A. et al. Optineurin links myosin VI to the Golgi complex and is involved in Golgi organization and exocytosis. *J Cell Biol* **169**, 285-295 (2005).
2. Combet, C., Blanchet, C., Geourjon, C. & Deleage, G. [NPS@](#): network protein sequence analysis. *Trends Biochem Sci* **25**, 147-50 (2000).
3. Morris, S.M. & Cooper, J.A. Disabled-2 colocalizes with the LDLR in clathrin-coated pits and interacts with AP-2. *Traffic* **2**, 111-23 (2001).
4. Mishra, S.K. et al. Disabled-2 exhibits the properties of a cargo-selective endocytic clathrin adaptor. *Embo J* **21**, 4915-26 (2002).
5. Pollard, T.D. & Borisy, G.G. Cellular motility driven by assembly and disassembly of actin filaments. *Cell* **112**, 453-65 (2003).
6. Weisman, L.S. Organelles on the move: insights from yeast vacuole inheritance. *Nat Rev Mol Cell Biol* **7**, 243-52 (2006).